Search for Lorentz and CPT Violation in Neutrino Sector

Nitheesh S Pillai

A dissertation to be submitted for the partial fulfilment of BS-MS dual degree in Science

Indian Institute of Science Education and Research, Mohali
May, 2020

Certificate of Examination

This is to certify that the dissertation titled **"Search for Lorentz and CPT Violation in Neutrino Sector"** submitted by **Mr. Nitheesh S Pillai (Reg. No. MS15089)** for the partial fulfilment of BS-MS dual degree programme of the Institute, has been examined by the thesis committee duly appointed by the Institute. The committee finds the work done by the candidate satisfactory and recommends that the report be accepted.

Dr. Vishal Bhardwaj Dr. Manabendra Bera Dr. Ambresh Shivaji

(Supervisor)

Dated: June 14, 2020

Declaration

The work presented in this dissertation has been carried out by me under the guidance of Dr. Ambresh Shivaji at the Indian Institute of Science Education and Research, Mohali.

This work has not been submitted in part or in full for a degree, a diploma, or a fellowship to any other university or institute. Whenever contributions of others are involved, every effort is made to indicate this clearly, with due acknowledgement of collaborative research and discussions. This thesis is a bonafide record of original work done by me and all sources listed within have been detailed in the bibliography.

Nitheesh S Pillai
(Candidate)

Dated: June 14, 2020

In my capacity as the supervisor of the candidate's project work, I certify that the above statements by the candidate are true to the best of my knowledge.

Dr. Ambresh Shivaji
(Supervisor)

Abstract

The Standard Model has been a well-celebrated achievement for the physicists. Although it is a successful theory, there are certain cases and phenomena which are beyond its scope. This issue demands the search for a more general theory. Lorentz and CPT violation in the neutrino sector is an area to look for new physics - physics beyond the Standard Model. This thesis project is an attempt to learn the scope of this route. The project focuses on Lorentz and CPT violating theories, their application to the neutrino physics (oscillation phenomena, to be precise), and ways to detect the violation parameters experimentally. We have reviewed the phenomena of neutrino oscillation and theory of neutrino masses. In the context of neutrino oscillation, various Lorentz and CPT violating models have been discussed. As an example, we have chosen Puma model, in paricular, c^8a^5m model to fit the experimentally observed neutrino oscillation data collected at MiniBooNE. In our analysis, we have fixed the neutrino mass and have varied CPT and Lorentz violating parameters c^8 and a^5. Our one-parameter analysis implies that 1σ allowed region for c^8 is $[2.16, 2.69] \times 10^{-16} GeV^{-4}$, while the corresponding region for a^5 is $[1.18, 1.71] \times 10^{-19} GeV^{-1}$.

Acknowledgement

I thank my project guide, Dr Ambresh Shivaji, for guiding me and giving me insights throughout my project. I would also like to thank a PhD scholar, Ms Nishat Fiza, for helping me with valuable inputs and for proofreading my thesis. I thank Dr Manabendra Bera and Dr Vishal Bharadwaj for giving feedback and approving my work. I am also thankful to my parents and friends for being highly supportive during my thesis project.

Contents

List of Tables

List of Figures

Chapter 1

Introduction

Our understanding of nature and its fundamental particles are far from complete. We are actively working to discover more and more. This effort led to an immensely successful theory - The Standard Model (SM) of particle physics. The particle physicist around the globe has widely celebrated this theory just because of how accurately it explains the particle nature and interaction. The latest incredible achievement being the discovery of the Higgs Boson.

Although this theory is very successful, certain phenomena and cases are existing in nature which it is not able to explain. Few examples are the existence of dark matter and the anomalous behaviour of neutrinos. We know such cases exist because we have experimental evidence. This "issue" forces us to look for a better and more "complete" theory. We need to look for some "new physics" - physics beyond the SM.

Search for new physics has been the interest of many in the recent years, and there have been several routes laid down such as Supersymmetry and String theory. However, one way to go about is by considering this - is it necessary that Lorentz symmetry must be obeyed? What happens if we relax this constraint? Will such theories be able to explain what SM could, as well as it couldn't?

That is precisely the route of our interest. Lorentz and CPT violating theories. One potential candidate to work with this theory is the neutrinos since their anomalous behaviour is a snake pit for the SM. A very interesting property of propagating neutrinos - the flavour

oscillation - would be particularly interesting to work. This project, thus, follows the path of Lorentz and CPT violating theories in the Neutrino sector.

Chapter 2

Neutrinos - History and progress

2.1 A brief history

A neutrino (ν) is a Standard Model lepton. They are unique since they have very distinctive properties from other particles. They are neutral and interact only via weak interactions. Their mass is several orders less than other fermions. Since they interact via weak interactions, it is challenging to understand their intrinsic properties. The existence of neutrinos was first postulated by W. Pauli in 1930, to justify the issue of obtaining a continuous energy spectrum in β-decay of atomic nuclei. He initially called this particle as "neutron". Pauli was very speculative of his proposal and did not publish his results until 1934. However, till this time, E. Fermi had already developed the theory of β-decay process. Fermi later renamed the particles to "Neutrino (Little neutral one)" (as a wordplay on neutrone, the Italian name of the neutron) to distinguish it from neutron (as we know today), discovered by J. Chadwick in 1932.

2.2 Detection and a new discovery

Since neutrinos interact mainly via weak interaction only, it isn't possible to probe them directly. So, its effects or consequences of its interaction with particles had to be observed to study them. Therefore, indirect detection techniques were developed. Today, there are

different kinds of detectors such as Scintillators, Radiochemical detectors, Cherenkov detectors, Radio detectors and calorimeter detectors.

The first detection of neutrinos was in 1954 by Clyde Cowan and Frederick Reines(Rajasekaran, 2016). They were able to detect the electron antineutrino flux coming from a nearby detector. Different methods were developed eventually.

These new experiments noticed a significant reduction in the flux of neutrinos when compared to the expected flux. These anomalies were first observed in cases of solar and atmospheric neutrinos. The first experiment to measure the solar neutrino flux "anomaly" was Ray Davis' Homestake experiment (1965). This experiment used radiochemical detection method and consisted of 400,000 litres of Perchloroethylene (C_2Cl_4). The reaction involved in the detection process is:

$$\nu_e + {}^{37}Cl \rightarrow {}^{37}Ar + e-$$

This reaction has a threshold of 0.814 MeV. Homestake experiment noted an average capture rate of solar neutrinos of 2.56 ± 0.25 SNU (1 SNU = 10^{-36} neutrino interactions per target atom per second). However Standard Solar Model predicted that Homestake should have seen about 8.1 ± 1.2 SNU. This was the birth of "Solar Neutrino Problem". Since the Homestake experiment had no information about directionality, the results were not widely accepted by the scientific community at that time.

Solar Neutrino Problem was only reconfirmed 20 years later when Super-Kamiokande in 1985 measured the solar neutrino flux again. They used Cerenkov detection process (about which we will discuss more in the coming chapters) and obtained clear amount of excess events in the direction of the Sun, confirming that the neutrinos detected were, in fact, solar neutrinos. Much similar to the Homestake Experiment, they also observed around 50% deficit in the neutrino flux. The experiment had a high threshold of 7.5 MeV.

After Super-Kamiokande (Super-K), it was clear that there was, in fact, some deficit in the solar neutrino flux. The first problem which was realized with these experiments was the high threshold of previous experiments. However, most of the neutrino flux was released at lower energies through the pp-chain in the Sun. So the previous experiments were insensitive to the majority of the solar neutrino flux. To cover-up for the Homestake

and S-Kamiokande, Gallium experiments were proposed. These experiments, because of their low threshold, were sensitive to most of the solar neutrino flux. Experiments such as SAGE and GALLEX (radiochemical detectors using Gallium as their main detector element) also observed a deficit in the neutrino flux.

After the unexpected neutrino flux measurements by the above-mentioned experiments, questions were raised whether the "Standard Solar Model", used to estimate solar neutrino flux, is correct or not. Helioseismology results turned the decision in favour of "Standard Solar Model" (SSM). The results were matching with the expectations to better than 99.5%. So, it was concluded that the problem might be in the detection experiments.

Researchers realized that the previous experiments had sensitivity exclusively to electron neutrinos only. So, it could be possible that they could be getting other flavours, but the experiment was unable to detect them. This led to the Sudbury Neutrino Observatory (SNO) detector experiment. SNO is a Cerenkov "Heavy-Water" detector. SNO used heavy water since deuteron is a very fragile nucleus. It only takes about 2 MeV to break it apart into a proton and a neutron. The deuterium in heavy water allows the detection of all types of neutrinos. SNO was able to detect neutrino via three different interactions (Rajasekaran, 2016),(Raychaudhuri, 2004):

- The Charged-Current (CC) channel: This reaction can only be initiated by electron neutrinos. Therefore, will detect the flux of electron neutrinos alone.

$$\nu_e + d \rightarrow p + p + e^-$$

- The Elastic Scattering (ES) channel: This channel is most sensitive to electron neutrinos. detects $\phi(\nu_e) + 0.15[\phi(\nu_\mu) + \phi(\nu_\tau)]$.

$$\nu_e + e^- \rightarrow \nu_e + e^-$$

- The Neutral Current (NC) channel: This channel is equally sensitive to all flavours of neutrinos. Hence, it measures the total flux $\phi(\nu_e) + \phi(\nu_\mu) + \phi(\nu_\tau)$.

$$\nu + d \rightarrow n + p + \nu$$

SNO used the measurements of these three independent reaction channels to get individual flux of neutrinos. Their measurement of the neutrino flux (in units of $10^{-8}cm^{-2}s^{-1}$) was:

$\phi_{cc} = \phi(\nu_e) = 1.76 \pm 0.01$

$\phi_{ES} = \phi(\nu_e) + 0.15[\phi(\nu_\mu) + \phi(\nu_\tau)] = 2.39 \pm 0.26$

$\phi_{NC} = \phi(\nu_e) + \phi(\nu_\mu) + \phi(\nu_\tau) = 5.09 \pm 0.63$

The total flux of muon and tau neutrinos from the Sun $\phi(\nu_\mu) + \phi(\nu_\tau)$ is $(3.33 \pm 0.63)10^{-8}cm^{-2}s^{-1}$. This is roughly three times larger than the flux of electron neutrino. We know that the Suno only produces electron neutrinos. This led to a remarkable conclusion - some neutrinos must change flavour as they travel from the Sun to the Earth. Further, the SSM predicts a total flux of neutrinos with energies greater than 2 MeV (the deuteron break-up energy) of $\phi_{SSM} = (5.05 \pm 1.01)10^{-8}cm^{-2}s^{-1}$, which is in very good agreement with the NC flux measured by SNO. Hence this led to one of the first evidence of a phenomenon known as "Neutrino Oscillation".

Such anomaly was also observed in case of the atmospheric neutrinos. The atmosphere is constantly bombarded by cosmic rays. Atmospheric neutrinos stem from the decay of the charged pions and subsequently muons, which are produced when the cosmic rays hit the air nuclei in the atmosphere. Neutrinos in atmosphere are predominantly produced in two flavors (ν_e, ν_μ). The decay chain is:

$$\pi^\pm \rightarrow \mu^\pm + \nu_\mu(\bar{\nu}_\mu)$$

$$\mu^\pm \rightarrow e^\pm + \bar{\nu}_\mu(\nu_\mu) + \nu_e(\bar{\nu}_e)$$

The flux of ν_e and ν_μ depends on the flux of muons produced in the decay of pi/K in the atmosphere. Hence the uncertainties on the flux of each of them are highly correlated. Therefore, even if uncertainties on the absolute flux are high, the ratio of ν-induced muon to electron events, for a given detector configuration, can be estimated more accurately. We have:

$$R_{theory}(E) = \frac{N_\mu^{exp}(E)}{N_e^{exp}(E)} \tag{2.1}$$

where $N_{\mu}^{exp}(E)$ and $N_{e}^{exp}(E)$ are the expected number of muons and electrons, respectively(Raychaudhuri, 2004). Here, E is the energy of the charged lepton produced in the interaction. The ratio R_{theory} is expected to be around 2 at low energies.

The spectrum of low energy ν-induced muons and electrons has been measured experimentally by various experiments (Soudan 2, MACRO and Super-Kamiokande) and compared with predictions. The ratio is defined as:

$$R_{obs}(E) = \frac{N_{\mu}^{obs}(E)}{N_{e}^{obs}(E)} \tag{2.2}$$

The ratio of (1) and (2) is called the "Double Ratio". It is given by:

$$R = \frac{R_{obs}(E)}{R_{theory}(E)} \tag{2.3}$$

This ratio is expected to be unity. However, various experiments showed that R varies significantly from unity. This observation was referred to as the "Atmospheric Neutrino Anomaly". Super-K was able to measure the direction of the incoming neutrinos in addition to the R-value. This detector, in addition to confirming anomaly with high statistics, also gave evidence of Neutrino Oscillation.

In the next chapter, we will delve deeper into the phenomena of Neutrino oscillations.

Chapter 3

Neutrino Oscillations

First proposed by Bruno Pontecorvo in 1957, experiments with neutrinos from various sources (solar, atmospheric, reactor and accelerator) have very well established that neutrinos produced in a well-defined flavour state (at the source) have a nonzero probability of being detected in a different flavour state. Neutrinos change flavour as they propagate. The neutrino of a specific flavour can be measured to have a different flavour later. This phenomenon is known as neutrino oscillation.

The probability of flavour change depends on the neutrino energy and the distance traversed between the source and the detector. The theory of neutrino oscillation was able to resolve the problem of discrepancy between the predicted flux of the solar (and the atmospheric) neutrinos and the observed flux. Another important fact is that if the theory has to hold, then the neutrinos must have mass since the probability of flavour change is also dependent on the mass-squared difference ($(\Delta m)^2$). Neutrino oscillation also tells that neutrino flavour states are linear combinations of the mass eigenstates, and therefore, these leptons must mix. The solar and atmospheric neutrino flavour changes can be described by different sets of oscillation parameters. Let us now look at general derivation.

3.1 General Derivation

The flavour eigenstates, ν_α, are linear combinations of the mass eigenstates ν_i (Kayser, 2008). Hence:

$$|\nu_\alpha >= \sum_{i=1}^{n} U^*_{\alpha k} |\nu_k > \tag{3.1}$$

where U is unitary matrix, α corresponds to flavour states and k is corresponds to mass eigenstates. These are the states at the source (i.e. $x = 0, t = 0$). Apply the propagation operator to the mass eigenstates:

$$|\nu_k(x,t) >= e^{-i\phi_k} |\nu_k(0,0) > \tag{3.2}$$

where $\phi_k = E_k t - p_k x$. Also, invert the mixing matrix to mass eigenstates as a superposition of flavour states.

$$|\nu_k >= \sum_\gamma U_{\gamma k} |\nu_\gamma >$$

Hence, we can write:

$$|\nu_\alpha(x.t) >= \sum_\gamma \sum_k U^*_{\alpha k} U_{\gamma k} e^{-i\phi_k} |\nu_k(x,t) > \tag{3.3}$$

The probability of getting flavour β at (x,t) if α is generated at the source is given by the square of the amplitude.

$$P_{\nu_\alpha(0,0) \to \nu_\beta(x,t)} = | < \nu_\alpha(0,0) | \nu_\beta(x,t) > |^2 \tag{3.4}$$

$$P_{\nu_\alpha \to \nu_\beta} = | \sum_k U^*_{\alpha k} U_{\beta k} e^{-i\phi_k} |^2 \tag{3.5}$$

This formula can be expanded to get:

$$P_{\nu_\alpha \to \nu_\beta} = \sum_{kj} U^*_{\alpha k} U_{\beta k} U_{\alpha j} U^*_{\beta j} exp[-i(\phi_k - \phi_j)] \tag{3.6}$$

We can now consider an approximation that neutrinos are ultra-relativistic and hence for any realistic energy (E), the rest mass (i.e. mass eigenvalue (m_i)) is very small in comparison to E. Hence,

$$p = \sqrt{E_i^2 - m_i^2} = E_i\sqrt{1 - \frac{m_i^2}{E_i^2}} \approx E_i(1 - \frac{m_i^2}{2E_i^2})$$

Since neutrinos are ultra-relativistic, we can replace t(c=1) by x (or L = Distance between source and detector). Using the above approximation, we get

$$P_{\nu_\alpha \to \nu_\beta} = \sum_{kj} U^*_{\alpha k} U_{\beta k} U_{\alpha j} U^*_{\beta j} exp[-i\frac{\Delta m^2_{kj} L}{2E}] \tag{3.7}$$

where $\Delta m^2_{kj} = m^2_k - m^2_j$.

Using the identity:

$$|z_1 + z_2 + z_3 + ...|^2 = \sum_k |z_k|^2 + 2Re \sum_{k>j} z_k z^*_j$$

we get,

$$P_{\nu_\alpha \to \nu_\beta} = \sum_k |U_{\alpha k}|^2 |U_{\beta k}|^2 + 2Re \sum_{k>j} U^*_{\alpha k} U_{\beta k} U_{\alpha j} U^*_{\beta j} exp[-2\pi i \frac{L}{L^{Osc}_{kj}}] \tag{3.8}$$

where L^{Osc}_{kj} =Oscillation Length $= \frac{4\pi E}{\Delta m^2_{kj}}$is the distance at which phase generated by Δm^2_{kj} becomes 2π.

We can also write the above equation in a different form using the following identity (obtained by squaring the condition on matrix elements of a unitary matrix):

$$\sum_k |U_{\alpha k}|^2 |U_{\beta k}|^2 = \delta_{\alpha\beta} - 2Re \sum_{k>j} U^*_{\alpha k} U_{\beta k} U_{\alpha j} U^*_{\beta j}$$

We get,

$$P_{\alpha\beta} = \delta_{\alpha\beta} - 4\sum_{k>j} Re[U^*_{\alpha k} U_{\beta k} U_{\alpha j} U^*_{\beta j}] \sin^2(\frac{\Delta m^2_{kj} L}{4E}) + 2\sum_{k>j} Im[U^*_{\alpha k} U_{\beta k} U_{\alpha j} U^*_{\beta j}] \sin(\frac{\Delta m^2_{kj} L}{2E}) \tag{3.9}$$

When $\alpha = \beta$, it is the "Survival Probability" and when $\alpha \neq \beta$, it is the "Transition Probability". For antineutrinos, we get a -2 factor instead of 2 in eq.(3.9).

Survival Probability is measured by "Disappearance Channel" i.e. we measure the fraction of neutrinos of original flavour left. On the other hand, Transition Probability is measured by "Appearance Channel" i.e. we measure the fraction of neutrinos of the new flavour.

3.2 2-Flavour Neutrino Oscillation

We will look at a simple case - let us consider two flavour states. Analysis done here helps to understand 3-flavour neutrino oscillations. Two flavour oscillation is described by one mixing angle (θ) and one mass difference. The flavour states and mass states are related to each other by a unitary matrix (U), which can be written as:

$$U = \begin{pmatrix} U_{\alpha 1} & U_{\alpha 2} \\ U_{\beta 1} & U_{\beta 2} \end{pmatrix} = \begin{pmatrix} \cos(\theta) & \sin(\theta) \\ -\sin(\theta) & \cos(\theta) \end{pmatrix}$$

Hence,

$$\begin{pmatrix} \nu_\alpha \\ \nu_\beta \end{pmatrix} = \begin{pmatrix} \cos(\theta) & \sin(\theta) \\ -\sin(\theta) & \cos(\theta) \end{pmatrix} \begin{pmatrix} \nu_1 \\ \nu_2 \end{pmatrix}$$

The transition probability can be obtained by using equation (3.9)

$$P_{\alpha\beta} = \sin^2(2\theta)\sin^2(\frac{\Delta m^2 L}{4E}) = \sin^2(2\theta)\sin^2(1.27\frac{\Delta m^2(eV^2)L(km)}{E(GeV)}) \tag{3.10}$$

The corresponding survival probability is given by:

$$P_{\alpha\alpha} = 1 - P_{\alpha\beta} \tag{3.11}$$

Since θ is a physical parameter, it is the amplitude determining part of $P_{\alpha\beta}$. On the other hand, Δm^2 is the frequency-determining part (Raychaudhuri, 2004).

3.2.1 Parameters

- Mixing Angle, θ
  - It determines how different are flavour states from mass states. If $\theta = 0$, it can be easily seen from mixing matrix form that flavour states are identical to mass states, that is, there is no mixing. If $\theta = \frac{\pi}{4}$, there's maximal mixing.
- Mass-squared difference, Δm^2
  - For non-zero oscillation probability, it is important for this factor to be non-zero. This implies that the neutrino mass eigenvalues must neither be zero nor degenerate. Also, $P_{\alpha\beta}$ is invariant under $\Delta m^2 \to -\Delta m^2$. Hence, we can't tell which neutrino mass is heavier.
- Baseline to Energy Ratio, L/E
  - This is the only parameter under the control of experimentalists. L is the distance between the source and the detector, and E is the energy of the neutrinos. Experimentally, if we suspect value of Δm^2, then we try to build the experiment to be maximally sensitive to the oscillation probability. Hence, the argument of sin should be integral multiple of $\pi/2$, i.e.,

$$1.27\Delta m^2 \frac{L}{E} = (2n+1)\frac{\pi}{2}$$

$$\Rightarrow \frac{L}{E} = \frac{\pi}{2.54\Delta m^2}$$

Therefore, the theory of neutrino oscillations demands the neutrinos to be massive. However, in the original Standard Model, the neutrinos are massless. Therefore, neutrino masses had to be incorporated into the Standard Model. Another issue is that the nature of neutrinos is unknown - we don't know if they are Dirac particles or Majorana particles. How to incorporate the neutrino masses? How do we interpret the masses? In the next chapter, we will focus on these topics.

Chapter 4

Neutrino Masses

Neutrino masses is one of the most important subjects of study in neutrino physics. We still don't clearly know the origin of neutrino masses. It is believed that neutrinos are nothing but a low-energy manifestation of physics beyond SM and high-energy scale suppression could be the reason why the neutrino masses are small. Theoretical methods have been worked out to explain the "smallness" of neutrino masses, such as various seesaw mechanisms (Akhmedov et al., 2000).

To incorporate the neutrino masses to the SM, we need to introduce the right-handed field, $\nu_{\alpha R}$ to the SM. We can then generate neutrino mass via the Higgs mechanism. This is a "minimally extended Standard Model". The right-handed fields do not interact via the weak interaction. These fields are singlets under the symmetries of the SM. Therefore, they are "sterile". They only participate in gravitational interaction. The left-handed neutrino fields are "active".

4.1 Dirac and Majorana Mass

In the unitary gauge, the Standard Model Higgs-lepton Yukawa Lagrangian is (Giunti and Kim, 2007):

$$\mathscr{L}_{H,L} = -\left(\frac{v+H}{\sqrt{2}}\right) \sum_{\alpha,\beta=e,\mu,\tau} Y'^{\ell}_{\alpha\beta} \overline{\ell'_{\alpha L}} \ell'_{\beta R} + H.c.$$

Where $Y'^{\ell}$is the Yukawa coupling matrix, ℓ' is the array of charged lepton fields, and $\alpha,\beta = e,\mu,\tau$.

$$\ell'_L = \begin{pmatrix} e'_L \\ \mu'_L \\ \tau'_L \end{pmatrix}, \ell'_R = \begin{pmatrix} e'_R \\ \mu'_R \\ \tau'_R \end{pmatrix}$$

Therefore, in matrix form, we can write,

$$\mathscr{L}_{H,L} = -\left(\frac{v+H}{\sqrt{2}}\right)\overline{\ell'_L}Y'^{\ell}\ell'_R + H.c.$$

This is modified by incorporating another term for neutrinos similar to the first term of the above equation.

$$\mathscr{L}_{H,L} = -\left(\frac{v+H}{\sqrt{2}}\right)\left[\overline{\ell'_L}Y'^{\ell}\ell'_R + \overline{\nu'_L}Y'^{\nu}\nu'_R\right] + H.c.$$

where $\nu'_L = \begin{pmatrix} \nu'_{eL} \\ \nu'_{\mu L} \\ \nu'_{\tau L} \end{pmatrix}$, $\nu'_R = \begin{pmatrix} \nu'_{eR} \\ \nu'_{\mu R} \\ \nu'_{\tau R} \end{pmatrix}$ and Y'^{ν} is neutrino Yukawa coupling matrix.

We can diagonalize Y'^{ℓ} and Y'^{ν} and eventually obtain the diagonalized Higgs-lepton Yukawa Lagrangian :

$$\mathscr{L}_{H,L} = -\left(\frac{v+H}{\sqrt{2}}\right)\left[\overline{\ell_L}Y^{\ell}\ell_R + \overline{n_L}Y^{\nu}n_R\right] + H.c.$$

$$= -\left(\frac{v+H}{\sqrt{2}}\right)\left[\sum_{\alpha=e,\mu,\tau} y^{\ell}_{\alpha}\overline{\ell_{\alpha L}}\ell_{\alpha R} + \sum_{k=1}^{3} y^{\nu}_{k}\overline{\nu_{kL}}\nu_{kR}\right] + H.c.$$

In the above cases, $Y^{\nu} = \mathrm{V}_{\mathrm{L}}^{\nu\dagger}Y'^{\nu}\mathrm{V}_{\mathrm{R}}^{\nu}$ and $Y^{\ell} = \mathrm{V}_{\mathrm{L}}^{\ell\dagger}Y'^{\ell}\mathrm{V}_{\mathrm{R}}^{\ell}$, where V_R^{ℓ}, V_R^{ν}, $V_L^{\ell}$and V_L^{ν} are unitary matrices.

Also,
$Y^{\ell}_{\alpha\beta} = y^{\ell}_{\alpha}\delta_{\alpha\beta}$ and $Y^{\ell}_{kj} = y^{\ell}_{k}\delta_{kj}$,
$n_L = \mathrm{V}_L^{\nu\dagger}\nu'_L$ and $n_R = \mathrm{V}_R^{\nu\dagger}\nu'_R$,
$\ell_L = \mathrm{V}_L^{\ell\dagger}\ell'_L$ and $\ell_R = \mathrm{V}_R^{\ell\dagger}\ell'_R$

Now, using Dirac neutrino fields,

$$\nu_k = \nu_{kL} + \nu_{kR}$$

and Dirac charged lepton fields,

$$\ell = \ell_{\alpha L} + \ell_{\alpha R}$$

we get,

$$\mathscr{L}_{H,L} = -\frac{1}{\sqrt{2}}\left(\sum_{\alpha=e,\mu,\tau} y^{\ell}_{\alpha}\nu\overline{\ell_{\alpha}}\ell_{\alpha} + \sum_{k=1}^{3} y^{\nu}_{k}\nu\overline{\nu_k}\nu_k + \sum_{\alpha=e,\mu,\tau} y^{\ell}_{\alpha}\overline{\ell_{\alpha}}\ell_{\alpha}H + \sum_{k=1}^{3} y^{\nu}_{k}\overline{\nu_k}\nu_k H\right)$$

So, we get the neutrino masses by

$$m_k = \frac{y^{\nu}_{k}\nu}{\sqrt{2}} \tag{4.1}$$

Here, $k = 1,2,3$.

This is the Dirac neutrino mass, where we consider the picture in which neutrinos are Dirac in nature.

The mass term for neutrinos can be written as:

$$\mathscr{L}_{mass} = -m\overline{\nu}\nu \tag{4.2}$$

Here $\nu = \nu_L + \nu_R$. Therefore, for Dirac neutrinos, eq.(4.2) becomes,

$$\mathscr{L}^{D}{}_{mass} = -m_D(\overline{\nu}_R\nu_L + \overline{\nu}_L\nu_R) = -m_D\overline{\nu}_R\nu_L + H.c. \tag{4.3}$$

If neutrinos are Majorana in nature, i.e., if the particle is its own antiparticle, then we go ahead and make few important changes.

Since we consider neutrinos to be Majorana, then the right-handed field, ν_R, becomes,

$$\nu_R = \nu^{c}_{L} = (\overline{\nu_L})^{T} \tag{4.4}$$

Using this, we get the Majorana mass term for ν_L,

$$\mathscr{L}^L{}_{mass} = -\frac{1}{2} m_L \overline{\nu_L^C} \nu_L + H.c. \tag{4.5}$$

Similarly, for ν_R, we get,

$$\mathscr{L}^R{}_{mass} = -\frac{1}{2} m_R \overline{\nu_R^C} \nu_R + H.c. \tag{4.6}$$

4.2 Dirac-Majorana Neutrino Mass Term

Although we know about the existence of ν_L, we don't know if ν_R exists. However, its existence is allowed by the symmetries of the SM. If only the former exists, then the Dirac mass term can't exist, and the neutrinos will be Majorana in nature. If both the fields exist, then the mass can have Dirac term contribution as well as Majorana term contribution from each field. Therefore, in general, neutrino lagrangian can contain Majorana mass term for $\nu_L$and ν_R, and the Dirac mass term (Giunti and Kim, 2007).

Therefore, the total Dirac-Majorana neutrino mass term is,

$$\mathscr{L}^{D+M}{}_{mass} = \mathscr{L}^D{}_{mass} + \mathscr{L}^L{}_{mass} + \mathscr{L}^R{}_{mass} \tag{4.7}$$

Therefore, we see that if neutrinos are Dirac particles, the mass can have contribution from both Dirac mass term and the Majorana mass term. This is one of the reasons which make neutrinos special compared to other fundamental particles.

4.3 Oscillation Parameters

In case of three-flavour oscillation, depending on the nature of neutrinos, the neutrino mixing matrix U (refer Chapter3) depends on more parameters.

If neutrinos are Dirac in nature, then the oscillation is governed by four parameters - three mixing angles ($\theta_{12}, \theta_{23}, \theta_{13}$), and a CP-violation phase (δ_{CP}).

The mixing matrix is known as the Pontecorvo-Maki-Nakagawa-Sakata matrix, or the PMNS matrix (Raychaudhuri, 2004), (Giunti and Kim, 2007). The most widely used parametrization is,

$$U = U_D = U_{PMNS} = \begin{bmatrix} 1 & 0 & 0 \\ 0 & c_{23} & s_{23} \\ 0 & -s_{23} & c_{23} \end{bmatrix} \begin{bmatrix} c_{13} & 0 & s_{13}e^{-i\delta_{CP}} \\ 0 & 1 & 0 \\ -s_{13}e^{i\delta_{CP}} & 0 & c_{13} \end{bmatrix} \begin{bmatrix} c_{12} & s_{12} & 0 \\ -s_{12} & c_{12} & 0 \\ 0 & 0 & 1 \end{bmatrix} \tag{4.8}$$

where, $s_{ij} = sin(\theta_{ij})$ and $c_{ij} = cos(\theta_{ij})$. In the case of Majorana neutrinos, the mixing matrix receives contribution from CP-violation phases of Majorana natures as well. Therefore, the mixing matrix becomes,

$$U = U_M = U^D D^M \tag{4.9}$$

Here, $D^M = diag(e^{-i\lambda_1}, e^{i\lambda_2}, e^{i\lambda_3})$, where λ_i are Majorana CP-violation phases. By convention, λ_1 is set to zero. Therefore, even if the Dirac CP-violation phase is absent, CP-violation can be observed as a result of the Majorana CP-violation phase contribution. An important thing to note is that all these parameters governing mixing aren't energy-dependent and can be independently chosen to match the data.

Chapter 5

Lorentz and CPT Violating Theories

Lorentz and CPT symmetries are the two most important symmetries which are conserved in the SM. However, these symmetries are "accidental symmetries", and not fundamental symmetries. In effect, a theory which respects stability and causality is acceptable, and therefore, a stable and causal theory which doesn't conserve the Lorentz symmetry would still be valid. The existing theory does face some stability issues at very high energies(Kostelecký and Lehnert, 2001). Moreover, conventional theories invoke additional hypothetical particles (such as sterile neutrinos) to explain certain "anomalies". This isn't elegant enough since we are introducing additional unknown parameters to explain some phenomenon. Therefore, we need to look for a more stable and complete theory. Possibly, relaxing the Lorentz symmetry might give us a more general theory which can explain processes which the SM couldn't.

5.1 A General Description

There are many ways to invoke Lorentz violation in theory. One of the ways is to introduce terms for Lorentz violation into the particle Lagrangian density. Such terms are generated by contracting the Lorentz violating coefficients with tensor operators. Since Lorentz violation effects are, in general, expected to be small, probably as a result of

Planck-suppressed effects, the Lorentz-violating(LV) operators can be treated as perturbations whenever needed (Kostelecký and Mewes, 2012). Since we will be dealing with neutrinos, let us work with general fermions.

Consider N spinor fields ψ_a, where a is the spinor flavour, and $a = 1,2,...N$. We combine N spinors ψ_a with their charge conjugates to get a $2N$-dimensional multiplet of spinors,

$$\Psi_A = \begin{pmatrix} \psi_a \\ \psi_a^C \end{pmatrix} \tag{5.1}$$

This is done to incorporate Majorana coupling. Here, A ranges over $2N$ values and Ψ obeys,

$$\Psi^C = \mathscr{C}\Psi$$

$$\mathscr{C} = \begin{pmatrix} 0 & 1 \\ 1 & 0 \end{pmatrix}$$

Now, we lay down a general Lagrange density incorporating Lorentz and CPT violation:

$$\mathscr{L} = \frac{1}{2}\overline{\Psi}_A(\gamma^\mu i\partial_\mu \delta_{AB} - M_{AB} + \hat{\mathscr{Q}}_{AB})\Psi_B + H.c. \tag{5.2}$$

Here, $\hat{\mathscr{Q}}_{AB}$ is 4×4 matrix in spinor space and $2N\times 2N$ matrix in flavour space. As mentioned before, this operator is treated perturbatively. We can write M_{AB} as

$$M_{AB} = m_{AB} + im_{5AB}\gamma_5 \tag{5.3}$$

Due to the hermiticity of $\mathscr{L}$. Here, both m and m_5 are hermitian matrices. Also,

$$m = \mathscr{C}m^T\mathscr{C}$$

$$m_5 = \mathscr{C}m_5^T\mathscr{C}$$

The spin part of the LV operator can be expanded in the basis of 16 Dirac matrices (γ_i) :

$$\hat{\mathscr{Q}}_{AB} = \sum \hat{\mathscr{Q}}^{I}_{AB}\gamma_I = \hat{\mathscr{S}}_{AB} + i\hat{\mathscr{P}}_{AB}\gamma_5 + \hat{\mathscr{V}}^{\mu}_{AB}\gamma_\mu + \hat{\mathscr{A}}^{\mu}_{AB}\gamma_5\gamma_\mu + \frac{1}{2}\hat{\mathscr{T}}^{\mu\nu}_{AB}\sigma_{\mu\nu} \tag{5.4}$$

The $\frac{1}{2}$ factor in the last term arises since $\sigma_{\mu\nu} = \gamma_\mu\gamma_\nu - \gamma_\nu\gamma_\mu$. Here, all $\hat{\mathscr{Q}}^{I}_{AB}$ are hermitian operators in the flavour space, which arises from the hermiticity of $\mathscr{L}$, and are derivative dependent, which can be expressed as follows:

$$\hat{\mathscr{Q}}^{I}_{AB} = \sum_{d=3}^{\infty} \hat{\mathscr{Q}}^{(d)I\alpha_1\alpha_2\ldots\alpha_{d-3}}_{AB} p_{\alpha_1} p_{\alpha_2}\cdots p_{\alpha_{d-3}}$$

where, $p_\mu = i\partial_\mu$. Here, d is the dimension of individual operators.

We incorporate $\hat{\mathscr{Q}}_{AB}$ as follows:

$$\gamma^\nu p_\nu \delta_{AB} - M_{AB} + \hat{\mathscr{Q}}_{AB} = \hat{\Gamma}_{AB} p_\nu - \hat{M}_{AB} \tag{5.5}$$

where,

$$\hat{\Gamma}_{AB} = \gamma^\nu \delta_{AB} + \hat{c}^{\mu\nu}_{AB}\gamma_\mu + \hat{d}^{\mu\nu}_{AB}\gamma_5\gamma_\mu + \hat{e}^{\nu}_{AB} + i\hat{f}^{\nu}_{AB}\gamma_5 + \frac{1}{2}\hat{g}^{\kappa\lambda\nu}_{AB}\sigma_{\kappa\lambda}$$

, and

$$\hat{M}_{AB} = m_{AB} + im_{5AB}\gamma_5 + \hat{m}_{AB} + i\hat{m}_{5AB}\gamma_5 + \hat{a}^{\mu}_{AB}\gamma_\mu + \hat{b}^{\mu}_{AB}\gamma_5\gamma_\mu + \frac{1}{2}\hat{H}^{\mu\nu}_{AB}\sigma_{\mu\nu}$$

By doing this, we are clearly introducing the effect of Lorentz violation into both propagation and the mass of the neutrinos. Here, five are dimensionless operators - $\hat{c}^{\mu\nu}_{AB}, \hat{d}^{\mu\nu}_{AB}, \hat{e}^{\nu}_{AB}, \hat{f}^{\nu}_{AB}$ and $\hat{g}^{\kappa\lambda\nu}_{AB}$.Out of these, the former two are CPT even, whereas the rest are CPT odd. This follows from the property that tensor densities with even number of indices are CPT-even, and those with odd indices are CPT-odd (Lehnert, 2016). The other operators are of mass dimension one. Here, $\hat{m}_{AB}, \hat{m}_{5AB}$ and $\hat{H}^{\mu\nu}_{AB}$ are CPT even, whereas $\hat{a}^{\mu}_{AB}$ and $\hat{b}^{\mu}_{AB}$ are CPT odd.

Since $\hat{\Gamma}_{AB}$ is contracted with p_ν in eq.(5.5), its individual operators will also be contracted with P_ν. Therefore, we define,

$$\hat{c}^{\mu}_{AB} = \hat{c}^{\mu\nu}_{AB} p_\nu, \quad \hat{d}^{\mu}_{AB} = \hat{d}^{\mu\nu}_{AB} p_\nu, \quad \hat{e}_{AB} = \hat{e}^{\nu}_{AB} p_\nu, \quad \hat{f}_{AB} = \hat{f}^{\mu}_{AB} p_\nu, \quad \hat{g}^{\kappa\lambda}_{AB} = \hat{g}^{\kappa\lambda\nu}_{AB} p_\nu$$

These "new" operators are related to the operators in eq.(5.4) as follows,

$$\begin{array}{lll} \hat{\mathscr{S}}_{AB} = \hat{e}_{AB} - \hat{m}_{AB} & \hat{\mathscr{P}}_{AB} = \hat{f}_{AB} - \hat{m}_{5AB} & \hat{\mathscr{V}}^{\mu}_{AB} = \hat{c}^{\mu}_{AB} - \hat{a}^{\mu}_{AB} \\ \hat{\mathscr{A}}^{\mu}_{AB} = \hat{d}^{\mu}_{AB} - \hat{b}^{\mu}_{AB} & \hat{\mathscr{T}}^{\mu\nu}{}_{AB} = \hat{g}^{\mu\nu}_{AB} - \hat{H}^{\mu\nu}_{AB} & \end{array} \tag{5.6}$$

Here, $\hat{\mathscr{S}}_{AB}, \hat{\mathscr{P}}_{AB}$ are CPT-even, whereas $\hat{\mathscr{V}}^{\mu}_{AB}, \hat{\mathscr{A}}^{\mu}_{AB}, \hat{\mathscr{T}}^{\mu}_{AB}$ are CPT-odd.

Since the Hamiltonian formulation is more convenient to work with, we will switch to Hamiltonian. Having Lorentz violation and concomitant higher-order time derivatives makes it difficult to construct the Hamiltonian. We can find an effective Hamiltonian ($2N \times 2N$) which will describe the physics at leading order.

We will start with the modified Dirac equation:

$$(p_\mu \gamma^\mu \delta_{AB} - M_{AB} + \hat{\mathscr{Q}}_{AB})\Psi_B = 0 \tag{5.7}$$

Now, we multiply by γ_0 from the left and define H_{AB} by the following condition:

$$(E\delta_{AB} - H_{AB})\Psi_B = \gamma_0(p_\mu \gamma^\mu \delta_{AB} - M_{AB} + \hat{\mathscr{Q}}_{AB})\Psi_B = 0$$

Here, $E = p_0$. Therefore, we have,

$$H_{AB} = \gamma_0(\boldsymbol{p}.\boldsymbol{\gamma}\delta_{AB} + M_{AB} - \hat{\mathscr{Q}}_{AB}) = (H_0)_{AB} + \delta H_{AB} \tag{5.8}$$

Here, $(H_0)_{AB} = \gamma_0(\boldsymbol{p}.\boldsymbol{\gamma}\delta_{AB} - M_{AB})$ with energy E_0 and $\delta H_{AB=} - \gamma_0\hat{\mathscr{Q}}_{AB}$, which is the LV perturbation.

5.2 General Lorentz Violating Theory for Neutrinos

We will be following the same framework mentioned in the previous section for neutrinos but will be implementing it onto the left-handed neutrino fields since the propagating neutrinos are left-handed and the right-handed field doesn't have any significant role.

For convenience, we introduce the left-handed and right-handed mass matrix $m_L$and m_R, such that $m_R = (m_L)^\dagger = m + im_5$. The neutrino mass matrix, therefore, becomes,

$$M = m_L P_L + m_R P_R$$

Here, $P_L$and P_R are chiral projection operators ($P_L = (1-\gamma_5)/2$ and $P_R = (1+\gamma_5)/2$). The right-handed mass matrix can be described with Dirac and Majorana type masses by:

$$m_R \mathscr{C} = \begin{pmatrix} L & D \\ D^T & R \end{pmatrix}$$

where, D is the Dirac-mass matrix, whereas L and R are the left-handed and right-handed Majorana mass matrix. All are $N \times N$matrices. R and L must be symmetric.

The usual equation describing the left-handed fermion in the absence of Lorentz-violation is

$$p.\gamma\psi_L - L\psi_L^C - D\psi_R = 0 \tag{5.9}$$

Here left-right neutrino mixing will vanish if $D = 0$. For $D \neq 0$, the seesaw mechanism is invoked to suppress mixing (a mechanism to explain neutrino masses) (Yanagida and Yoshimura, 1980)(Mohapatra and Senjanović, 1980), which requires assuming R to be large. Right-handed field fermion is described by

$$p.\gamma\psi_R^C - R\psi_R - D^T\psi_L^C = 0 \tag{5.10}$$

For large R, $\psi_R \approx -R^{-1}D^T\psi_L^C$. Therefore, left-handed field equation becomes,

$$p.\gamma\psi_L - (L - DR^{-1}D^T)\psi_L^C = 0 \tag{5.11}$$

Here, we define effective mass m_l:

$$m_l = L - DR^{-1}D^T \tag{5.12}$$

Therefore, the previous equation becomes

$$p.\gamma\psi_L - m_l\psi_L^C = 0 \tag{5.13}$$

We take the left-handed projection of the Hamiltonian. It will give a good approximation to study the observed behaviour of neutrino. The projection becomes:

$$H_L = \begin{pmatrix} P_L & 0 \\ 0 & P_R \end{pmatrix} H \begin{pmatrix} P_L & 0 \\ 0 & P_R \end{pmatrix} \tag{5.14}$$

This can be expressed as an operator acting on two-component Weyl spinors. This required defining $\sigma^\mu = (\sigma^0, \sigma^j)$, where σ^j are the three Pauli matrices and σ^0 is the identity matrix (2×2). Now, the adjoint matrix becomes $\bar{\sigma} = (\sigma^0, -\sigma^j)$. The Weyl spinor will be denoted by ϕ which are associated with Dirac spinors $P_L\psi$. In this representation, we will suppress flavour indices. H_L is replaced by Weyl form H_W, and Ψ is replaced by

$$\Phi_W = \begin{pmatrix} \phi \\ \phi^C \end{pmatrix}$$

Here, $\phi^C = i\sigma^2\phi^*$. Eq (34) becomes

$$p.\bar{\sigma}\phi - m_l\phi^C = 0 \tag{5.15}$$

The unperturbed Hamiltonian $(H_W)_0$ becomes

$$(H_W)_0 = \begin{pmatrix} -\boldsymbol{p}.\boldsymbol{\sigma} & m_l \\ m_l^\dagger & \boldsymbol{p}.\boldsymbol{\sigma} \end{pmatrix} \tag{5.16}$$

The LV Hamiltonian δH becomes

$$\delta H_W = \begin{pmatrix} -\hat{\mathscr{V}}_L^\mu \bar{\sigma}_\mu & -\hat{\mathscr{S}}_L - \frac{i}{2}\hat{\mathscr{T}}_M^{\mu\nu}\bar{\sigma}_\mu\sigma_\nu \\ -\hat{\mathscr{S}}_L - \frac{i}{2}(\hat{\mathscr{T}}_M^{\mu\nu})^\dagger\sigma_\mu\bar{\sigma}_\nu & (-1)^{(d+1)}\hat{\mathscr{V}}_L^{\mu T}\sigma_\mu \end{pmatrix} \tag{5.17}$$

Here, subscript L indicates the left-handedness. Chirality preservation makes sure that right-handed components are absent. The full Hamiltonian is $H_W = (H_W)_0 + \delta H_W$.

This can be block diagonalized with suitable approximation. We can either proceed by treating neutrinos to be relativistic or nonrelativistic. We will consider the former case, and block diagonalize the full Hamiltonian to the order m_l^2 using the transformation

$$U = \begin{pmatrix} 1 - \frac{m_l m_l^\dagger}{8\boldsymbol{p}^2} & -\frac{m_l \boldsymbol{p}.\boldsymbol{\sigma}}{2\boldsymbol{p}^2} \\ \frac{m_l^\dagger \boldsymbol{p}.\boldsymbol{\sigma}}{2\boldsymbol{p}^2} & 1 - \frac{m_l^\dagger m_l}{8\boldsymbol{p}^2} \end{pmatrix} \tag{5.18}$$

Therefore the unperturbed Hamiltonian becomes,

$$(H'_W)_0 = U(H_W)_0 U^\dagger = \begin{pmatrix} -\boldsymbol{p}.\boldsymbol{\sigma}\left(1 + \frac{m_l m_l^\dagger}{2\boldsymbol{p}^2}\right) & 0 \\ 0 & \boldsymbol{p}.\boldsymbol{\sigma}\left(1 + \frac{m_l^\dagger m_l}{2\boldsymbol{p}^2}\right) \end{pmatrix} \tag{5.19}$$

Weyl doublet Φ_W transforms,

$$\Phi'_W = U\Phi_W = \begin{pmatrix} \phi' \\ (\phi')^C \end{pmatrix}$$

Now, we need to find the effective hamiltonian h_{eff} governing the neutrino propagation. So, we expand Φ'_W in helicity components:

$$\phi' = [A(t,\boldsymbol{p})e^{i\boldsymbol{x}.\boldsymbol{p}} + B^*(t,\boldsymbol{p})e^{-i\boldsymbol{x}.\boldsymbol{p}}]\mathscr{E}_{\boldsymbol{p}},$$
$$(\phi')^C = [A^*(t,\boldsymbol{p})e^{-i\boldsymbol{x}.\boldsymbol{p}} + B(t,\boldsymbol{p})e^{i\boldsymbol{x}.\boldsymbol{p}}]\mathscr{E}^{\boldsymbol{C}}_{\boldsymbol{p}},$$

Here, $\mathscr{E}_{\boldsymbol{p}}$ is a normalized negative-helicity spinor, which satisfies the condition $\boldsymbol{p}.\boldsymbol{\sigma}\,\mathscr{E}_{\boldsymbol{p}} = -|\boldsymbol{p}|\mathscr{E}_{\boldsymbol{p}}$. Amplitudes $A(t,\ \boldsymbol{p})$ and $B(t,\ \boldsymbol{p})$ are associated with negative-helicity ν and positive-helicity $\bar{\nu}$. Positive energy part of Schrodinger equation in the Lorentz-invariant limit gives,

$$i\frac{\partial}{\partial t}\begin{pmatrix} A \\ B \end{pmatrix} = (h_{eff})_0 \begin{pmatrix} A \\ B \end{pmatrix}$$

Here,

$$(h_{eff})_0 = |\boldsymbol{p}|\begin{pmatrix} 1 & 0 \\ 0 & 1 \end{pmatrix} + \frac{1}{2|\boldsymbol{p}|}\begin{pmatrix} m_l m_l^\dagger & 0 \\ 0 & m_l^\dagger m_l \end{pmatrix} \tag{5.20}$$

This is the unperturbed effective Hamiltonian for ν and $\overline{\nu}$ amplitudes in the Lorentz-invariant limit.

We diagonalize δH_W to obtain the LV contribution δh:

$$\delta H'_W = U\delta H_W U^\dagger = \delta H_W + [\delta U, \delta H_W] + O(m_l^2) \tag{5.21}$$

Here,

$$\delta U = \frac{\boldsymbol{p}.\boldsymbol{\sigma}}{2\boldsymbol{p}^2}\begin{pmatrix} 0 & -m_l \\ m_l^\dagger & 0 \end{pmatrix}$$

As before, we get δh by positive-energy projection,

$$\delta h = \begin{pmatrix} \mathscr{E}_{\boldsymbol{p}}^\dagger & 0 \\ 0 & \mathscr{E}_{\boldsymbol{p}}^{C\dagger} \end{pmatrix} \delta H'_W \begin{pmatrix} \mathscr{E}_{\boldsymbol{p}} & 0 \\ 0 & \mathscr{E}_{\boldsymbol{p}}^{C} \end{pmatrix} \tag{5.22}$$

We can use the following identities for getting explicit result:

$$\begin{aligned} \mathscr{E}_{\boldsymbol{p}}^\dagger \overline{\sigma}_\mu \mathscr{E}_{\boldsymbol{p}} &= \mathscr{E}_{\boldsymbol{p}}^{C\dagger} \sigma_\mu \mathscr{E}_{\boldsymbol{p}}^{C} \approx \tfrac{p_\mu}{|\boldsymbol{p}|}, \\ \mathscr{E}_{\boldsymbol{p}}^\dagger \sigma_\mu \mathscr{E}_{\boldsymbol{p}}^{C} &= -\mathscr{E}_{\boldsymbol{p}}^\dagger \overline{\sigma}_\mu \mathscr{E}_{\boldsymbol{p}}^{C} = \sqrt{2}\varepsilon_\mu, \\ \mathscr{E}_{\boldsymbol{p}}^{C\dagger} \sigma_\mu \mathscr{E}_{\boldsymbol{p}} &= -\mathscr{E}_{\boldsymbol{p}}^{C\dagger} \overline{\sigma}_\mu \mathscr{E}_{\boldsymbol{p}} = \sqrt{2}\varepsilon_\mu^*, \end{aligned}$$

Here, the polarization vector $\varepsilon^\mu$is

$$\varepsilon^\mu = \frac{1}{\sqrt{2}}(0; \hat{\boldsymbol{e}}_1 + i\hat{\boldsymbol{e}}_2)$$

and $\varepsilon_\mu(-\boldsymbol{p}) = \varepsilon_\mu^*(\boldsymbol{p})$. Also $\hat{\boldsymbol{e}}_1, \hat{\boldsymbol{e}}_2$ are arbitrary unit vectors and are chosen in a way such that $\hat{\boldsymbol{p}}$, $\hat{\boldsymbol{e}}_1$, $\hat{\boldsymbol{e}}_2$ form a right-handed orthonormal triad. Comparing this with the spherical-coordinate unit vectors indicates that the spatial part of ε^μ is the helicity unit vector $\hat{\varepsilon}_+$ discussed in the scope of LV test with photons and LV in electrodynamics (check Appendix A2 of (Kostelecký and Mewes, 2008);(Kostelecký and Mewes, 2009)).

Proceeding in the above route shows that to the order of $O(m_l)$, the LV part of effective Hamiltonian becomes,

$$\delta h = \frac{1}{|\boldsymbol{p}|}\begin{pmatrix} \hat{a}_{eff} - \hat{c}_{eff} & -\hat{g}_{eff} + \hat{H}_{eff} \\ -\hat{g}^{\dagger}_{eff} + \hat{H}^{\dagger}_{eff} & -\hat{a}^{T}_{eff} - \hat{c}^{T}_{eff} \end{pmatrix} \tag{5.23}$$

These LV operators are effective operators which consist of individual LV operators. The experiments are more sensitive to the combined effect of the individual LV operators. Hence, we defined these effective operators. The diagonal blocks govern neutrino-neutrino mixing, whereas the off-diagonal blocks govern neutrino-antineutrino mixing. $\hat{a}_{eff}$ and $\hat{g}_{eff}$ are CPT-odd, whereas $\hat{c}_{eff}$ and $\hat{H}_{eff}$ are CPT even, and have the following forms:

$$\hat{a}_{eff} = p_\mu \hat{a}^{\mu}_{L} - \hat{e}_1 + 2i\varepsilon_\mu \varepsilon^{*}_{\nu} \hat{g}^{\mu\nu}_{l} \tag{5.24}$$

$$\hat{g}_{eff} = i\sqrt{2} p_\mu \varepsilon_\nu \hat{g}^{\mu\nu}_{M+} + \sqrt{2}\varepsilon_\mu \hat{a}^{\mu}_{l} \tag{5.25}$$

$$\hat{c}_{eff} = p_\mu \hat{c}^{\mu}_{L} - \hat{m}_1 + 2i\varepsilon_\mu \varepsilon^{*}_{\nu} \hat{H}^{\mu\nu}_{l} \tag{5.26}$$

$$\hat{H}_{eff} = i\sqrt{2} p_\mu \varepsilon_\nu \hat{H}^{\mu\nu}_{M+} + \sqrt{2}\varepsilon_\mu \hat{c}^{\mu}_{l} \tag{5.27}$$

Here, each quantity $\hat{\mathscr{B}}^{\mu\nu}_{M+} = \frac{1}{2}(\hat{\mathscr{B}}^{\mu\nu} + i\tilde{\hat{\mathscr{B}}}^{\mu\nu})$ and follows the identity $\varepsilon_\mu \varepsilon_\nu \hat{\mathscr{B}}^{\mu\nu}_{\mu M+} \backsimeq -p^j \hat{\mathscr{B}}^{0j}_{M+}/|\boldsymbol{p}|$.

$\hat{a}^{\mu}_{L}, \hat{c}^{\mu}_{L}, \hat{g}^{\mu\nu}_{M+}$ and $\hat{H}^{\mu\nu}_{M+}$ are independent of mass matrix m_l:

$$\begin{aligned} \hat{a}^{\mu}_{L} &= \hat{a}^{\mu}_{D} + \hat{b}^{\mu}_{D} \qquad\qquad ; \hat{c}^{\mu}_{L} = \hat{c}^{\mu}_{D} + \hat{d}^{\mu}_{D} \\ \hat{g}^{\mu\nu}_{M+} &= \tfrac{1}{2}(\hat{g}^{\mu\nu}_{M} + i\tilde{\hat{g}}^{\mu\nu}_{M}) \quad ; \hat{H}^{\mu\nu}_{M+} = \tfrac{1}{2}(\hat{H}^{\mu\nu}_{M} + i\tilde{\hat{H}}^{\mu\nu}_{M}) \end{aligned} \tag{5.28}$$

Here, the subscripts D and M refer to the Dirac and Majorana types. These obey the following conditions:

$$\begin{aligned} \hat{a}^{\mu}_{L} &= (\hat{a}^{\mu}_{L})^{\dagger}; \quad \hat{g}^{\mu\nu}_{M+} = i\tilde{\hat{g}}^{\mu\nu}_{M+} = (\hat{g}^{\mu\nu}_{M+})^{T} \\ \hat{c}^{\mu}_{L} &= (\hat{c}^{\mu}_{L})^{\dagger}; \quad \hat{H}^{\mu\nu}_{M+} = i\tilde{\hat{H}}^{\mu\nu}_{M+} = -(\hat{H}^{\mu\nu}_{M+})^{T} \end{aligned} \tag{5.29}$$

The remaining operators are linear in m_l:

$$\begin{aligned}
\hat{m}_l &= \tfrac{1}{2}[(\hat{m}_M + i\hat{m}_{5M})m_l^\dagger + m_l(\hat{m}_M + i\hat{m}_{5M})^\dagger] \\
\hat{a}_l^\mu &= \tfrac{1}{2}[\hat{a}_L^\mu m_l + m_l(\hat{a}_L^\mu)^T] \\
\hat{c}_l^\mu &= \tfrac{1}{2}[\hat{c}_L^\mu m_l + m_l(\hat{c}_L^\mu)^T] \\
\hat{e}_l &= \tfrac{1}{2}[(\hat{e}_M + i\hat{f}_M)m_l^\dagger + m_l(\hat{e}_M + i\hat{f}_M)^\dagger] \\
\hat{g}_l^{\mu\nu} &= \tfrac{1}{2}[\hat{g}_{M+}^{\mu\nu} m_l^\dagger + m_l(\hat{g}_{M+}^{\mu\nu})^\dagger] \\
\hat{H}_l^{\mu\nu} &= \tfrac{1}{2}[\hat{H}_{M+}^{\mu\nu} m_l^\dagger + m_l(\hat{H}_{M+}^{\mu\nu})^\dagger]
\end{aligned} \tag{5.30}$$

and they obey the following conditions:

$$\begin{aligned}
&\hat{a}_l^\mu = (\hat{a}_l^\mu)^T, && \hat{c}_l^\mu = -(\hat{c}_l^\mu)^T, \\
&\hat{m}_l = \hat{m}_l^\dagger, \quad \hat{e}_l = \hat{e}_l^\dagger, && \hat{g}_l^{\mu\nu} = (\hat{g}_l^{\mu\nu})^\dagger, \quad \hat{H}_l^{\mu\nu} = (\hat{H}_l^{\mu\nu})^\dagger
\end{aligned}$$

The complete effective Hamiltonian is,

$$h_{eff} = (h_{eff})_0 + \delta h \tag{5.31}$$

5.2.1 Spherical Decomposition

Search for Lorentz violation generally depends on looking for anisotropies related to rotation symmetry violation. Therefore, decomposing the Lorentz violation coefficients in spherical harmonics will be useful. In fact, this is a more convenient option when compared to utilizing the rotational transformation property of LV coefficients.

We can expand the $p_\mu$dependent pieces in (5.23) of δh in spherical harmonics. Since the terms in diagonal block of the LV effective hamiltonian are rotational scalars, they can be expanded using $Y_{jm} \equiv_0 Y_{jm}$ (standard spherical harmonics). If we take the case of contribution involving coefficients $\hat{a}_L^\mu$, it can be expanded as,

$$p_\mu(\hat{a}_L^\mu) = \sum_{djmn} E^{d-2-n}|\boldsymbol{p}|^n Y_{jm}(\hat{\boldsymbol{p}})(c_L^{(d)})_{njm}^{ab}$$

Here, we consider the approximation $E \backsimeq |\boldsymbol{p}|$ to second order in small m_l. This is valid since we are working with Lorentz violation to first order in m_l. Similarly, other coefficients can also be expanded (Kostelecký and Mewes, 2012).

However, these coefficients contribute only via the four combinations (5.24, 5.25, 5.26, 5.27), and the experiments are more sensitive to these combinations, it makes more sense to utilize the expansions for these terms. These are-

$$\begin{aligned}
\hat{a}^{ab}_{eff} &= \sum |\boldsymbol{p}|^{d-2} Y_{jm}(\hat{\boldsymbol{p}}) (a^{(d)}_{eff})^{ab}_{jm} \\
\hat{c}^{ab}_{eff} &= \sum |\boldsymbol{p}|^{d-2} Y_{jm}(\hat{\boldsymbol{p}}) (c^{(d)}_{eff})^{ab}_{jm} \\
\hat{g}^{ab}_{eff} &= \sum |\boldsymbol{p}|^{d-2}{}_{+1} Y_{jm}(\hat{\boldsymbol{p}}) (g^{(d)}_{eff})^{ab}_{jm} \\
\hat{H}^{ab}_{eff} &= \sum |\boldsymbol{p}|^{d-2}{}_{+1} Y_{jm}(\hat{\boldsymbol{p}}) (H^{(d)}_{eff})^{ab}_{jm}
\end{aligned} \tag{5.32}$$

And these set of combination term coefficients are a function of the fundamental coefficients :

$$\begin{aligned}
(a^{(d)}_{eff})^{ab}_{jm} &= (a^{(d)}_{L})^{ab}_{jm} - (e^{(d+1)}_{l})^{ab}_{jm} + (g^{(d+1)}_{l})^{ab}_{jm} \\
(c^{(d)}_{eff})^{ab}_{jm} &= (c^{(d)}_{L})^{ab}_{jm} - (m^{(d+1)}_{l})^{ab}_{jm} + (H^{(d+1)}_{l})^{ab}_{jm} \\
(g^{(d)}_{eff})^{ab}_{jm} &= (g^{(d)}_{M+})^{ab}_{jm} + (a^{(d+1)}_{l})^{ab}_{jm} \\
(H^{(d)}_{eff})^{ab}_{jm} &= (H^{(d)}_{M+})^{ab}_{jm} + (c^{(d+1)}_{l})^{ab}_{jm}
\end{aligned} \tag{5.33}$$

Properties of these spherical coefficients under discrete transformation can be found in Table II of (Kostelecký and Mewes, 2012).

Chapter 6

Lorentz and CPT Violating Models

The general LV theory involves many independent components, and working with all of them at the same time can become cumbersome. Therefore, it is better to come up with models focussing on specific parts such as modelling signals that could be associated with Lorentz and CPT violation. This is also important for the experiments as it helps in targeted experimental studies.

There are many Lorentz and CPT violation models that have been proposed. We will discuss some cases briefly to understand how constraints are implemented. One important point to note is that we have considered all the LV coefficients to be spacetime constants for energy and momentum conservation (Kostelecký and Mewes, 2012),(Díaz and Kostelecký, 2012). Please note that we will be suppressing the flavour indices for simplicity.

6.1 Massless Models

As the name suggests, these models work in the massless limit $m \to 0$. These models show that oscillation can occur even if the neutrinos are massless - oscillations can arise from CPT and Lorentz violation alone. These models can also be used in the ultrarelativistic limit.

Due to the massless limit, all the mass-induced coefficients (with subscript l) will vanish. Therefore, the LV effective hamiltonian (5.23) becomes,

$$\delta h = \frac{1}{|\boldsymbol{p}|}\begin{pmatrix} p_\mu \hat{a}_L^\mu - p_\mu \hat{c}_L^\mu & -i\sqrt{2}p_\mu \varepsilon_\nu \hat{g}_{M+}^{\mu\nu} + i\sqrt{2}p_\mu \varepsilon_\nu \hat{H}_{M+}^{\mu\nu} \\ -(i\sqrt{2}p_\mu \varepsilon_\nu \hat{g}_{M+}^{\mu\nu})^\dagger + (i\sqrt{2}p_\mu \varepsilon_\nu \hat{H}_{M+}^{\mu\nu})^\dagger & -(p_\mu \hat{a}_L^\mu)^T - (p_\mu \hat{c}_L^\mu)^T \end{pmatrix} \tag{6.1}$$

and effective coefficients reduces to,

$$(a_{eff}^{(d)})_{jm}^{ab} = (a_L^{(d)})_{jm}^{ab}$$

$$(c_{eff}^{(d)})_{jm}^{ab} = (c_L^{(d)})_{jm}^{ab}$$

$$(g_{eff}^{(d)})_{jm}^{ab} = (g_{M+}^{(d)})_{jm}^{ab}$$

$$(H_{eff}^{(d)})_{jm}^{ab} = (H_{M+}^{(d)})_{jm}^{ab}$$

The properties of spherical coefficients for massless models are given in Table 6.2.

These models are of interest because they show that phenomenon like neutrino oscillation alone cannot be used to claim that the neutrinos have mass.

Models such as Bicycle model (Alan Kostelecký and Mewes, 2004) have been widely studied. These models explain the oscillations very well. However, none of the existing models is completely successful. One of the major issues is the inability to simultaneously explain KamLAND data (Araki et al., 2005) and the observed shape of solar neutrino spectrum (Bellini et al., 2010) in the energy range 1-20 MeV.

However, the inclusion of direction-dependent coefficients hasn't been explored much. Most of the models exclude the effect of direction-dependent operators. Exploring those could be a possible route to achieve a completely valid massless model.

6.2 Flavour-blind Models

These models are 'blind' to flavour differences. This is achieved by setting the assumption that Lorentz and CPT violation and the mass-squared matrix affect all the flavours in the

Table 6.1: Spherical coefficients for massless models

Coefficient	d	j	number
$(a_L^{(d)})_{jm}^{ab}$	odd, ≥ 3	$d-2 \geq j \geq 0$	$9(d-1)^2$
$(c_L^{(d)})_{jm}^{ab}$	even, ≥ 4	$d-2 \geq j \geq 0$	$9(d-1)^2$
$(g_{M+}^{(d)})_{jm}^{ab}$	even, ≥ 4	$d-2 \geq j \geq 1$	$12d(d-2)$
$(H_{M+}^{(d)})_{jm}^{ab}$	odd, ≥ 3	$d-2 \geq j \geq 1$	$6d(d-2)$

same way. Although not realistic in terms of what we know about neutrinos, these models can be used to study neutrino propagation.

The effective hamiltonian for flabour-blind model, say, h_{eff}^{fb} decouples into three identical equations, and the coefficients $H_{M+}, H_l, e_{l,}$ vanish since H_{M+}, e_M, f_M are antisymmetric in flavour space. Therefore, the hamiltonian reduces to,

$$h_{eff}^{fb} = |\boldsymbol{p}| + \frac{|m_l|^2}{2|\boldsymbol{p}|} - \frac{\hat{c}_{eff}}{|\boldsymbol{p}|} + \frac{1}{|\boldsymbol{p}|}\begin{pmatrix} \hat{a}_{eff} & -\hat{g}_{eff} \\ -\hat{g}_{eff}^* & -\hat{a}_{eff} \end{pmatrix} \tag{6.2}$$

Even though diagonal elements are non-zero, neutrino oscillation is not observed since the flavours cannot be differentiated. However, the off-diagonal elements are still non-zero, and therefore, results in neutrino-antineutrino mixing.

(41) can be diagonalized using U to get the eigenvalues

$$E_{\pm}^{fb} = |\boldsymbol{p}| + \frac{|m_l|^2}{2|\boldsymbol{p}|} - \frac{\hat{c}_{eff}}{|\boldsymbol{p}|} + \frac{\lambda}{|\boldsymbol{p}|} \tag{6.3}$$

where $\lambda = \sqrt{\hat{a}_{eff}^2 + |\hat{g}_{eff}|^2}$

Here, $U = \begin{pmatrix} C & -S \\ S^* & C \end{pmatrix}$ having $C = \sqrt{\frac{\lambda+\hat{a}_{eff}}{2\lambda}}$ and $S = \frac{\hat{g}_{eff}}{\sqrt{2\lambda(\lambda+\hat{a}_{eff})}}$.

Things can be simplified further - restricting the neutrino-antineutrino mixing completely by setting $\hat{g}_{eff}$ to zero. This results in what is known as "Oscillation-free" models.

Table 6.3 shows the properties of coefficients for flavour-blind models (subscript "fb") and oscillation-free models (subscript "of").

Table 6.2: Spherical coefficients for flavour-blind and oscillation-free models

Coefficient	d	j	number
$(a_{fb}^{(d)})_{jm}$	odd, ≥ 3	$d-1 \geq j \geq 0$	d^2
$(c_{fb}^{(d)})_{jm}$	even, ≥ 4	$d-2 \geq j \geq 0$	$(d-1)^2$
$(g_{fb}^{(d)})_{jm}$	even, ≥ 2	$d-1 \geq j \geq 1$	$2(d^2-1)$
$(a_{of}^{(d)})_{jm}$	odd, ≥ 3	$d-2 \geq j \geq 0$	$(d-1)^2$
$(c_{of}^{(d)})_{jm}$	even, ≥ 4	$d-2 \geq j \geq 0$	$(d-1)^2$

6.3 Isotropic Models

These models are constructed by focussing on operators that obey rotational symmetry. Such models become well-defined only after its preferred inertial frame (of the observer) is specified, as the observer boosts mix with rotation. Therefore, all observers boosted with respect to this frame will observe anisotropic effects.

Although simple in design, these models can be utilized to study realistic effects. One important class of isotropic models is the Puma models (DÃaz and KosteleckÃœ, 2011), which we will be discussing more.

Chapter 7

Puma Models

Class of Puma models is of our interest because it is simple, yet powerful enough to perform complex studies. A compelling reason to explore these models is their success with just three parameters. The conventional model (3νSM) utilizes five parameters (refer chapter 4) and still fails to explain certain neutrino anomalies, whereas these models explain the oscillations as well as the anomalies with just three parameters. We will be specifically focussing on 3×3 effective Hamiltonian h^{ν}_{eff} which will govern the oscillations of three flavours of left-handed neutrinos. They have two important properties: zero eigenvalue and isotropic Lorentz violation (Díaz and Kostelecký, 2012). The zero eigenvalue can be attributed to a discrete symmetry of h^{ν}_{eff}. Isotropic Lorentz violation means that the boost invariance is broken while the rotations are intact.

Therefore, the Hamiltonian is independent of the direction of the momentum of the neutrinos. However, they have unconventional neutrino energy (E) dependence (Kostelecký and Mewes, 2009). This will lead to some interesting observations.

7.1 General Model

For the general model, the effective hamiltonian is of the form,

$$h^{v}_{eff} = A\begin{pmatrix} 1 & 1 & 1 \\ 1 & 1 & 1 \\ 1 & 1 & 1 \end{pmatrix} + B\begin{pmatrix} 1 & 1 & 1 \\ 1 & 0 & 0 \\ 1 & 0 & 0 \end{pmatrix} + C\begin{pmatrix} 1 & 0 & 0 \\ 0 & 0 & 0 \\ 0 & 0 & 0 \end{pmatrix} \tag{7.1}$$

Here, A, B, C are functions of E. $A = \frac{m^2}{2E}$, where m is the neutrino mass. B and C have unconventional energy dependence. A decreases inversely with E, whereas B and C increase with E (Díaz and Kostelecký, 2012).

The eigenvalue of the effective hamiltonian turns out to be,

$$\begin{aligned} \lambda_1 &= \tfrac{1}{2}[3A + B + C - \sqrt{(A-B-C)^2 + 8(A+B)^2}] \\ \lambda_2 &= \tfrac{1}{2}[3A + B + C + \sqrt{(A-B-C)^2 + 8(A+B)^2}] \\ \lambda_3 &= 0 \end{aligned} \tag{7.2}$$

The mixing matrix for diagonalizing effective hamiltonian can be expressed as,

$$U_{a'a} = \begin{pmatrix} \frac{\lambda_1 + 2A}{N_1} & \frac{A+B}{N_1} & \frac{A+B}{N_1} \\ \frac{\lambda_2 + 2A}{N_2} & \frac{A+B}{N_2} & \frac{A+B}{N_2} \\ 0 & \frac{-1}{\sqrt{2}} & \frac{1}{\sqrt{2}} \end{pmatrix} \tag{7.3}$$

where, $a^{'} = 1, 2, 3$ and $a = e, \mu, \tau$. The normalization factors are,

$$\begin{aligned} N_1 &= \sqrt{(\lambda_1 - 2A)^2 + 2(A+B)^2} \\ N_2 &= \sqrt{(\lambda_2 - 2A)^2 + 2(A+B)^2} \end{aligned} \tag{7.4}$$

The same for antineutrinos can be obtained by CPT conjugation of B and C.

Another important characteristic of this model is the Lorentz-violation seesaw (Alan Kostelecký and Mewes, 2004) mechanism that mimics a mass term at higher energies without invoking mass. The ratio of the LV coefficients acts like mass at higher energies.

We will take B and E to be monomials. Let us consider that they are of the form:

$$B(E) = \mathring{k}^{(p)} E^{p-3}, \quad C(E) = \mathring{c}^{(q)} E^{q-3} \tag{7.5}$$

where p, q are dimensions of the operators associated with $\mathring{k}^{(p)}$ and $\mathring{c}^{(p)}$.

Since the elements of h^{ν}_{eff} are all real, the oscillation probability from ν_b to ν_a can be written as,

$$P_{\nu_b \to \nu_a} = \delta_{ab} - 4 \sum_{a'>b'} U_{a'a} U_{a'b} U_{b'a} U_{b'b} sin^2(\Delta_{a'b'} L/2) \tag{7.6}$$

Here, $\Delta_{a'b'} = \lambda_{a'} - \lambda_{b'}$ and L is the baseline. Also, A, B, C are real. Therefore, all the processes are T invariant. This implies that CP violation can appear if and only if there is CPT violation.

7.2 c_8a_5m Model

For our study, we will be focussing on the c_8a_5m Puma model (DÃaz and KosteleckÃœ, 2011). Here, $\mathring{k}^{(p)} \equiv \mathring{a}^{(5)}$ and $\mathring{c}^{(q)} = \mathring{c}^{(8)}$. Some other variants of Puma models were also explored in the process, such as the c_4a_3m and the c_6c_4m model. However, the former fails to produce a signal in short baseline experiments since C (eq. 7.5) grows only linearly with energy, whereas the latter doesn't incorporate CPT violation since it only consists of CPT-even parameters. The c_8a_5m model performed very well in explaining the oscillation, as well as many anomalous phenomena in short and long-baseline experiments simultaneously.

Parameter values are chosen to match the results with experimental data. The value of the parameters which is widely accepted and provide excellent agreement with the experimental results are-

$$\begin{aligned} m^2 &= 2.6 \times 10^{-23} GeV^2 \\ \mathring{a}^{(5)} &= -2.5 \times 10^{-19} GeV^{-1} \\ \mathring{c}^{(8)} &= 1.0 \times 10^{-16} GeV^{-4} \end{aligned} \tag{7.7}$$

Here, $\mathring{a}^{(5)}$ is the source for CPT violation since it is CPT-odd. Its non-zero value implies that this model accommodates CPT violation. The value of m is chosen to be consistent with the limit from direct mass measurements and cosmological bounds (and, 2010). In this model, $a^{(5)}$ and $c^{(8)}$ are the only LV coefficients defined in an isotropic frame F_I. This frame can be any universal inertial frame, such as the cosmic microwave background (CMB).

The experiment frame, say F_E, is boosted in it by some combination of Earth's revolution about the Sun, its own rotation, and its motion relative to CMB. These LV coefficients then generate anisotropic effects via a net boost in F_I (Díaz and Kostelecký, 2012).

An important thing to note is that unlike the three-flavour-SM neutrino oscillation (refer Chapter 4) where the mixing angles were independent of energy, the mixing angles governing oscillations are dependent on A, B, C, and therefore, energy. The energy dependence of mixing matrix U also implies that the oscillation amplitude is now energy-dependent, which wasn't the case in the conventional model (since oscillation amplitude depends on mixing angle, which is energy-independent in the conventional model - refer Chapter 3).

Chapter 8

Analysis with c_8a_5m Model

Next step was to understand how the model worked. So, we started by looking at how the oscillation probability looked. We decided to set baseline $L = 500m$, which is that of MiniBooNE. The oscillation probability for $\nu_\mu \to \nu_e$ was calculated from eq. (7.6) and plotted.

After obtaining the plot for oscillation probability, the next step was to try using this model to understand if it could explain an experimental result.We chose the MiniBooNE experiment for this analysis. MiniBooNE (Mini Booster Neutrino Experiment) neutrino detector is a short-baseline Mineral oil-Cherenkov neutrino detector which was started to observe $\nu_\mu \to \nu_e$ oscillations. As mentioned before, the baseline is ~$500m$. The excess in electron-like events in MiniBooNE (Aguilar-Arevalo et al., 2009) was chosen for this. Fermilab reported a significant excess in the appearance of ν_e (at $\nu_\mu \to \nu_e$ channel) , in the energy range of $300MeV - 500MeV$.

From the published work, it was known that after all the cuts and removal of background contribution, ~ 380 relevant events were recorded. Plotting events with respect to energy utilizing the c_8a_5m model with the above input and the parameters in (7.7) revealed that there was a significantly higher occurrence in the energy region where excess was observed in the experiment.

This plot, however, utilized globally accepted parameter values. One should be able to determine parameter values from the experimental data. So, the data from the MiniBooNE

Figure 8.1: The event excess observed in MiniBooNE experiment (Aguilar-Arevalo et al., 2009).

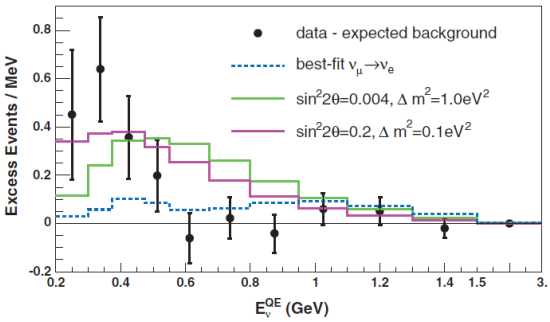

Table 8.1: MiniBooNE Data utilized for Parameter Estimation (Aguilar-Arevalo et al., 2009)

Event Sample	Data	Background	Excess Events
$200-300MeV$	232	186.8 ± 26.0	45.2 ± 26.0
$300-475MeV$	312	228.3 ± 24.5	83.7 ± 24.5
$475-1250MeV$	408	385.9 ± 35.7	22.1 ± 35.7

experiment was utilized for estimating the best fit parameter values for the MiniBooNE data (Table 8.1).

The analysis adopted was χ^2 function minimization by keeping two parameters fixed and varying one parameter. This was done for parameters $a^{(5)}$ and $c^{(8)}$, respectively. The χ^2function is defined as:

$$\chi^2 = \sum_i \frac{1}{\sigma_i^2}(N_{i,obs} - N_{i,theory})^2$$

Where, $N_{i,obs}$and $N_{i,theory}$ are observed and the theoretical data points, and σ_i are the errors associated with the data points.

First case was varying $a^{(5)}$ by fixing $c^{(8)}$and m^2. Values for latter two was, again, fixed as per (7.7). The χ^2 values were obtained, with which the minima (χ^2_{min}) and standard deviation ($\delta\chi^2$) was calculated and plotted (fig. 8.2).

χ^2_{min} was obtained for $a^{(5)} = 1.47 \times 10^{-19} GeV^{-1}$. The value for $\chi^2_{min} = 6.74 \times 10^2$ and $\delta\chi^2 = 1077.27$. From the plot, we see that the 1σ allowed range for the value of $a^{(5)} = [1.18, 1.71] \times 10^{-19} GeV^{-1}$.

Figure 8.2: χ^2 vs $a^{(5)}$. The line represents $\chi^2_{min} + \delta\chi^2$.

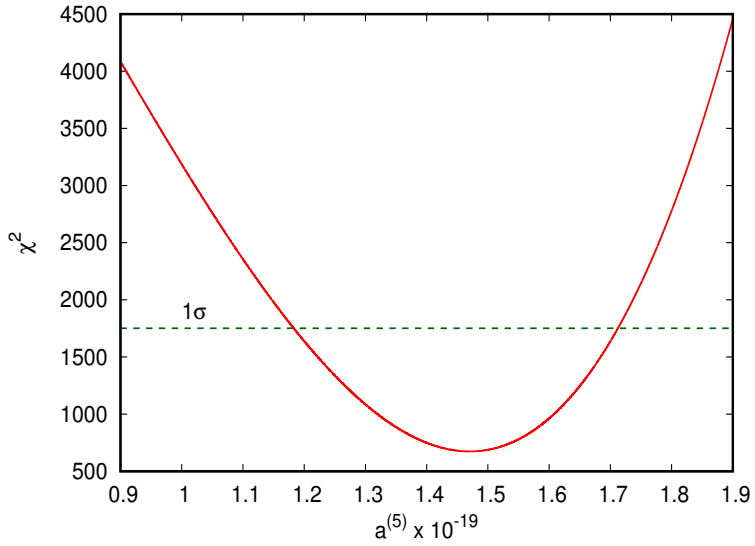

Next case was varying $c^{(8)}$ by fixing $a^{(5)}$and m^2. Values for latter two was, again, fixed as per (7.7). Just as before, the χ^2 values were obtained, with which the minima (χ^2_{min}) and standard deviation ($\delta\chi^2$) was calculated and plotted (fig. 8.3).

χ^2_{min} was obtained for $c^{(8)} = 2.37 \times 10^{-16} GeV^{-4}$. The value for $\chi^2_{min} = 4.29 \times 10^2$ and $\delta\chi^2 = 239.69$. From the plot, we see that the 1σ allowed range for the value of $c^{(8)} = [2.16, 2.69] \times 10^{-16} GeV^{-4}$.

The analysis can be taken forward to two-parameter analysis by utilizing region plots to obtain the best fit values for $a^{(5)}$ and $c^{(8)}$ simultaneously, while fixing m^2. One possible long-term outcome could be a package that can take in any LV models and estimate the best fit values for its LV parameters using the experimental data.

Figure 8.3: χ^2 vs $c^{(8)}$. The line represents $\chi^2_{min} + \delta\chi^2$.

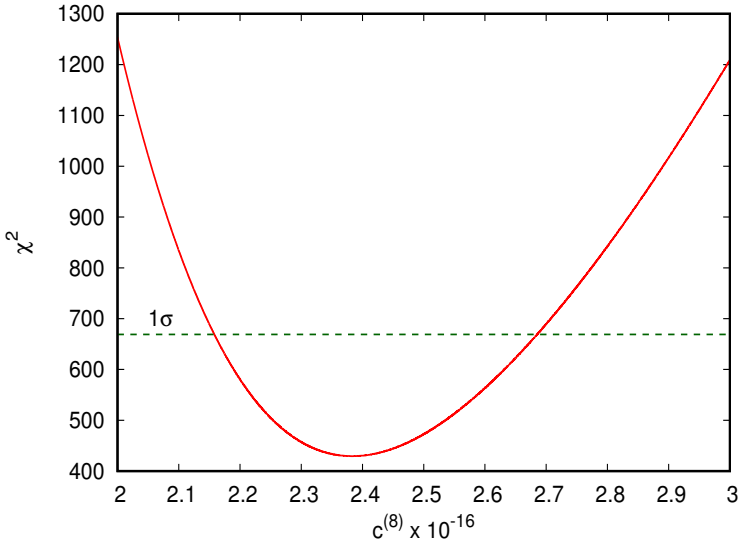

Conclusion

In this work, we have reviewed the standard phenomena of neutrino oscillation and have studied the effect of Lorentz violating parameters. In presence of Lorentz violating parameters, the neutrino oscillation is possible even if the neutrino masses are zero. Among many models of CPT and Lorentz violation, we have focussed on the Puma model to explain the observed excess in events at MiniBooNE. Within Puma model, we have chosen c^8a^5m model for our analysis based on χ^2 minimization.

This new route for searching for new physics is exciting and quite promising. There is a lot of potential in exploring the possibility of Lorentz and CPT violation and their consequences. We saw that phenomenon like oscillation could occur even if neutrinos were massless and therefore, demands for more concrete evidence. Similarly, the Puma model being very successful in explaining anomalies in neutrino experiments is an indication of the potential LV theories hold.

Bibliography

AGUILAR-AREVALO, A. A. AND ANDERSON, *et al.*, 2009. Unexplained excess of electronlike events from a 1-gev neutrino beam. *Phys. Rev. Lett.*, 102 (Mar 2009), 101802. doi:10.1103/PhysRevLett.102.101802. https://link.aps.org/doi/10.1103/PhysRevLett.102.101802.

AKHMEDOV, E.; BRANCO, G.; AND REBELO, M., 2000. Seesaw mechanism and structure of neutrino mass matrix. *Physics Letters B*, 478, 1 (2000), 215 – 223. doi:https://doi.org/10.1016/S0370-2693(00)00282-3. http://www.sciencedirect.com/science/article/pii/S0370269300002823.

ALAN KOSTELECKÝ, V. AND MEWES, M., 2004. Lorentz and cpt violation in neutrinos. *Phys. Rev. D*, 69 (Jan 2004), 016005. doi:10.1103/PhysRevD.69.016005. https://link.aps.org/doi/10.1103/PhysRevD.69.016005.

AND, K. N., 2010. Review of particle physics. *Journal of Physics G: Nuclear and Particle Physics*, 37, 7A (jul 2010), 075021. doi:10.1088/0954-3899/37/7a/075021. https://doi.org/10.1088%2F0954-3899%2F37%2F7a%2F075021.

ARAKI, T.; EGUCHI, K.; AND ENOMOTO, *et al.*, 2005. Measurement of neutrino oscillation with kamland: Evidence of spectral distortion. *Phys. Rev. Lett.*, 94 (Mar 2005), 081801. doi:10.1103/PhysRevLett.94.081801. https://link.aps.org/doi/10.1103/PhysRevLett.94.081801.

BELLINI, G. AND BENZIGER, *et al.*, 2010. Measurement of the solar ^{8}B neutrino rate with a liquid scintillator target and 3 mev energy threshold in the borexino detector. *Phys. Rev.*

D, 82 (Aug 2010), 033006. doi:10.1103/PhysRevD.82.033006. https://link.aps.org/doi/10.1103/PhysRevD.82.033006.

DÃAZ, J. S. AND KOSTELECKÃŒ, V. A., 2011. Three-parameter lorentz-violating texture for neutrino mixing. *Physics Letters B*, 700, 1 (2011), 25 – 28. doi:https://doi.org/10.1016/j.physletb.2011.04.049. http://www.sciencedirect.com/science/article/pii/S0370269311004485.

DÍAZ, J. S. AND KOSTELECKÝ, V. A., 2012. Lorentz- and *cpt*-violating models for neutrino oscillations. *Phys. Rev. D*, 85 (Jan 2012), 016013. doi:10.1103/PhysRevD.85.016013. https://link.aps.org/doi/10.1103/PhysRevD.85.016013.

GIUNTI, C. AND KIM, C. W., 2007. *Fundamentals of neutrino physics and astrophysics*. Oxford university press.

KAYSER, B., 2008. Neutrino oscillation phenomenology.

KOSTELECKỲ, V. A. AND LEHNERT, R., 2001. Stability, causality, and lorentz and cpt violation. *Physical Review D*, 63, 6 (2001), 065008.

KOSTELECKÝ, V. A. AND MEWES, M., 2008. Astrophysical tests of lorentz and CPT violation with photons. *The Astrophysical Journal*, 689, 1 (nov 2008), L1–L4. doi:10.1086/595815. https://doi.org/10.1086%2F595815.

KOSTELECKÝ, V. A. AND MEWES, M., 2009. Electrodynamics with lorentz-violating operators of arbitrary dimension. *Phys. Rev. D*, 80 (Jul 2009), 015020. doi:10.1103/PhysRevD.80.015020. https://link.aps.org/doi/10.1103/PhysRevD.80.015020.

KOSTELECKÝ, V. A. AND MEWES, M., 2012. Neutrinos with lorentz-violating operators of arbitrary dimension. *Phys. Rev. D*, 85 (May 2012), 096005. doi:10.1103/PhysRevD.85.096005. https://link.aps.org/doi/10.1103/PhysRevD.85.096005.

LEHNERT, R., 2016. Cpt symmetry and its violation. *Symmetry*, 8, 11 (2016), 114.

MOHAPATRA, R. N. AND SENJANOVIĆ, G., 1980. Neutrino mass and spontaneous parity nonconservation. *Phys. Rev. Lett.*, 44 (Apr 1980), 912–915. doi:10.1103/PhysRevLett.44.912. https://link.aps.org/doi/10.1103/PhysRevLett.44.912.

RAJASEKARAN, G., 2016. The story of the neutrino. *arXiv preprint arXiv:1606.08715*, (2016).

RAYCHAUDHURI, A., 2004. Neutrino oscillations: A solution to anomalies in observations of solar, atmospheric and laboratory neutrinos. In *Proc. Indian Natl. Sci. Acad., A*, vol. 70, 179–188.

YANAGIDA, T. AND YOSHIMURA, M., 1980. Various Schemes of Neutrino Mixing. *Progress of Theoretical Physics*, 64, 5 (11 1980), 1870–1873. doi:10.1143/PTP.64.1870. https://doi.org/10.1143/PTP.64.1870.